

Optical Double-Photon Absorption in CdS†

R. BRAUNSTEIN AND N. OCKMAN
RCA Laboratories, Princeton, New Jersey
 (Received 6 December 1963)

Observations have been made of the two-photon excitation of an electron from the valence to the conduction band in CdS ($E_g=2.5$ eV) using a pulsed ruby laser ($\hbar\omega=1.78$ eV). The radiative recombination emission from exciton and impurity levels subsequent to the simultaneous absorption of two quanta of $\hbar\omega=1.78$ eV was observed as a function of laser intensity and compared to the emission excited by single-quanta absorption for photons of $\hbar\omega>E_g$. It was found that the intensity of the recombination radiation is proportional to I_0^n for single-quanta excitation and I_0^{2n} for double-quanta excitation, where I_0 is the excitation intensity and n is a constant which differs for different groups of emission lines. The observed cross section for double-quanta excitation is compared with theory utilizing the band parameters of CdS.

I. INTRODUCTION

AN intrinsic semiconductor normally does not exhibit any optical absorption capable of producing electron-hole pairs for photon energies less than the energy gap. This is true for the light intensities employed in conventional optical absorption experiments. However, for sufficiently high incident intensities of photons whose energy is less than the band gap, the multiple-photon excitation of a valence electron to the conduction band can take place and consequently in principle, a perfectly transparent semiconductor does not exist! This type of transition involves virtual states and does not require the presence of impurity levels within the forbidden gap. In the present work,¹ a study has been made of the creation of electron-hole pairs in CdS by the simultaneous absorption of two photons produced by a focused ruby laser whose photon energy ($\hbar\omega=1.78$ eV) is considerably less than the CdS band gap ($E_g=2.5$ eV). The absorption was detected by observing the subsequent recombination emission produced in the region between 4900 and 5500 Å. The experimental results are compared with a theory which takes the band structure into account.

The advent of intense monochromatic sources of radiation by means of optical masers has made it experimentally feasible to observe a number of intensity-dependent optical interactions in matter which involve two or more photons. Harmonic generation²⁻⁷ and optical mixing,^{3,7} in which two photons of the same or

nearly the same frequency combine in a solid to produce a third photon, have been extensively studied. The observation of the above interactions in appropriate solids depends intimately upon the coherence of the incident light; in contrast double-photon absorption can in principle be observed with a conventional intense incoherent-light source. Since double-photon excitation depends upon the square of the incident intensity, this intrinsic absorption process is to be considered whenever a solid is irradiated with an intense light source of photon energies greater than half the band gap.

CdS was selected for the present study of double-photon absorption primarily because the single-photon absorption process has been extensively studied in this substance and it is consequently possible to compare double- and single-photon absorption on the same crystal. In addition, one can utilize the band-structure parameters determined from single-photon absorption measurements to estimate the double-photon absorption coefficients. We believe that this is the first observation of a simultaneous two-photon transition between valence and conduction bands in a semiconductor. Previously, two-photon absorption has been observed between broad bands in (CaF₂:Eu²⁺)⁸ and in several polycyclic, aromatic, molecular crystals,^{9,10} as well as between discrete atomic levels in Cs vapor.¹¹ Recently, intensity-induced optical absorption has also been observed in a number of liquids.¹²

II. CALCULATION OF TWO-PHOTON ABSORPTION

The general theory for two-photon absorption was first given by Göppert-Mayer.¹³ The absorption coefficient for two-photon excitation of an electron from the valence to the conduction band in terms of the band-structure parameters in a semiconductor has been

† Supported as part of Project DEFENDER under the joint sponsorship of the Advanced Research Projects Agency, the Office of Naval Research, U. S. Navy, the U. S. Department of Defense and RCA Laboratories, Princeton, New Jersey.

¹ A preliminary report of this work was presented at a meeting of the American Physical Society, 1963 [Bull. Am. Phys. Soc. 8, 30 (1963)].

² P. A. Franken, A. E. Hill, C. W. Peters, and G. Weinreich, Phys. Rev. Letters 7, 118 (1961).

³ M. Bass, P. A. Franken, A. E. Hill, C. W. Peters, and G. Weinreich, Phys. Rev. Letters 8, 18 (1962).

⁴ J. A. Giordmaine, Phys. Rev. Letters 8, 19 (1962).

⁵ P. D. Maker, R. W. Terhune, M. Nisenoff, and C. M. Savage, Phys. Rev. Letters 8, 21 (1962).

⁶ R. W. Terhune, P. D. Maker, and C. M. Savage, Phys. Rev. Letters 8, 404 (1962).

⁷ A. Savage and R. C. Miller, Appl. Opt. 1, 661 (1962).

⁸ W. Kaiser and C. G. B. Garrett, Phys. Rev. Letters 7, 229 (1961).

⁹ L. Peticolas, J. P. Goldsborough, and K. E. Rieckhoff, Phys. Rev. Letters 10, 43 (1963).

¹⁰ S. Singh and B. P. Stoicheff, J. Chem. Phys. 38, 2032 (1963).

¹¹ I. D. Abella, Phys. Rev. Letters 9, 453 (1962).

¹² J. A. Giordmaine and J. A. Howe, Phys. Rev. Letters 11, 207 (1963).

¹³ M. Göppert-Mayer, Ann. Phys. (Paris) 9, 273 (1931).

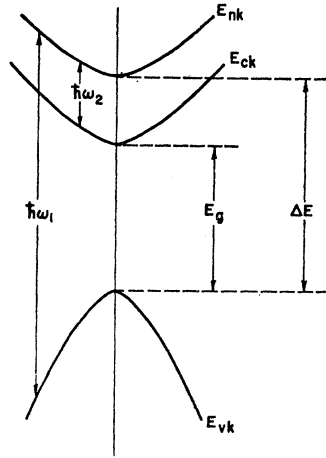


FIG. 1. Schematic diagram of band structure model used to calculate double-photon absorption.

derived by Braunstein¹⁴ and extended by Loudon¹⁵ to take into account the effect of excitons on the absorption coefficient close to the band edge. Two-photon excitation of impurity levels in a crystal has been considered by Kleinman.¹⁶ The theory for photoelectric emission from a metal surface by two-photon absorption has been considered by Smith.¹⁷ For continuity of discussion and comparison of the present experiments with theory, the band-to-band calculations for allowed transitions¹⁴ will be rederived and the calculations extended to the case of forbidden transitions.

For simplicity, consider a solid whose band structure consists of a valence and two conduction bands with extrema at $\mathbf{k}=0$; a schematic diagram of this model is shown in Fig. 1. If two monochromatic beams of energies $\hbar\omega_1$ and $\hbar\omega_2$ both less than the band gap but whose sum is greater than the gap are incident upon such a solid, the transition probability per unit time for an electron to be excited from an initial valence-band state \mathbf{k} to a final conduction-band state \mathbf{k} by simultaneously absorbing two photons is given by

$$\begin{aligned} p_{vk,ck} = \frac{2\pi}{\hbar} & \left| \frac{H_{vn}H_{nc}}{[\Delta E + E_{nk} + E_{vk} - \hbar\omega_1]} \right. \\ & \left. + \frac{H_{vn}H_{nc}}{[\Delta E + E_{nk} + E_{vk} - \hbar\omega_2]} \right|^2 \\ & \times \delta(E_g + E_{ck} + E_{vk} - \hbar\omega_1 - \hbar\omega_2), \quad (1) \end{aligned}$$

where H_{vn} and H_{nc} are the optical matrix elements which couple the valence band and conduction band, respectively, to an intermediate state n . E_g is the separation of the valence and lower conduction bands at $\mathbf{k}=0$, ΔE is the separation between the valence- and intermediate-band extrema and E_{ck} , E_{nk} , and E_{vk} are the

energies in the conduction band, intermediate band, and valence band, respectively, as measured from their extrema. In the above expression only transitions between states with the same \mathbf{k} are considered; i.e., vertical transitions, and consequently, the finite momentum of the photon was neglected. If one includes the fact that the optical matrix elements do not vanish for arbitrarily small photon wave vectors, one could use a two-band model for the calculation. In the present calculation, we have considered only one virtual state, while in fact it is usually necessary to sum over all possible intermediate states. The justification for this procedure is that the dominant contribution to the transition probability results from intermediate states which are closest to the final conduction band.

The absorption coefficient K_1 for photon $\hbar\omega_1$ when $\hbar\omega_1$ and $\hbar\omega_2$ are simultaneously present, may be simply related to the number of $\hbar\omega_1$ photons absorbed per unit time per unit volume and is given by

$$K_1 = -\frac{2n}{c} \frac{1}{N_1} \frac{\partial N_1}{\partial t} = +\frac{2n}{cN_1} \sum_k p_{vk,ck}, \quad (2)$$

where n is the index of refraction, c the velocity of light and N_1 the density of photons $\hbar\omega_1$. The factor of two is included in the absorption coefficient to account for the two-electron spin orientations. We shall assume that there is very little spatial variation of the beam within the medium, i.e., all absorption processes are small.

By combining Eqs. (1) and (2), the absorption coefficient is given by

$$\begin{aligned} K_1 = \frac{16\pi^3 n \hbar e^4}{cm^4 \omega_1 \omega_2} \int \frac{d^3k}{(2\pi)^3} & \left[\frac{P_{vn}^1 P_{nc}^2}{[\Delta E + E_{nk} + E_{vk} - \hbar\omega_1]} \right. \\ & \left. + \frac{P_{vn}^2 P_{nc}^1}{[\Delta E + E_{nk} + E_{vk} - \hbar\omega_2]} \right]^2 \\ & \times \delta(E_g + E_{ck} + E_{vk} - \hbar\omega_1 - \hbar\omega_2), \quad (3) \end{aligned}$$

where the conventional optical matrix elements¹⁸ have been used. P_{vn} and P_{nc} are the appropriate momentum matrix elements with superscripts 1 and 2 indicating their components in the directions of polarization of photons $\hbar\omega_1$ and $\hbar\omega_2$, respectively.

To obtain explicit expressions of K_1 for a given solid, it is necessary to have some knowledge of the momentum matrix elements as well as the \mathbf{k} dependence of E_{vk} , E_{nk} , and E_{ck} . If the transitions are allowed, i.e., the coupling is between bands of opposite parity, $|P_{vn}|^2$ and $|P_{nc}|^2$ can be taken as constants near the band edges as a first approximation and are given in terms of the f value for the transition by:

$$|P_{if}|^2 = m\hbar\omega_{if} f_{if} / 2. \quad (4)$$

¹⁴ R. Braunstein, Phys. Rev. **125**, 475 (1962).

¹⁵ R. Loudon, Proc. Phys. Soc. (London) **80**, 952 (1962).

¹⁶ D. A. Kleinman, Phys. Rev. **125**, 87 (1962).

¹⁷ R. L. Smith, Phys. Rev. **128**, 2225 (1962).

¹⁸ W. Heitler, *The Quantum Theory of Radiation* (Oxford University Press, New York, 1954), 2nd ed.

If the transitions are forbidden, i.e., between bands of the same parity, one may assume that the momentum matrix elements are proportional to \mathbf{k}_i of the initial state:

$$|P_{if}|^2 = (m/m_T)^2 \hbar^2 (\mathbf{e}_q \cdot \mathbf{k}_i)^2, \quad (5)$$

where m_T is an effective mass for the transition and \mathbf{e}_q represents a unit vector for the photon polarization.¹⁹ We shall assume that the energy bands are spherical and parabolic and consequently are given by

$$E_{vk} = \alpha_v \hbar^2 \mathbf{k}^2 / 2m, \quad E_{nk} = \alpha_n \hbar^2 \mathbf{k}^2 / 2m, \quad E_{ck} = \alpha_c \hbar^2 \mathbf{k}^2 / 2m, \quad (6)$$

where the α 's are the inverse effective-mass ratios.

There are three types of double-photon transitions to be considered depending upon the symmetries of the valence, conduction, and virtual-conduction bands. These may be defined as "allowed-allowed," "forbidden-allowed," and "forbidden-forbidden" transitions; the designations following from the appropriate matrix elements involved in the transitions. Substituting expressions, (4), (5), and (6) into Eq. (3) and performing the integrations, we obtain explicit expressions for the three possible types of transitions:

"allowed-allowed";

$$K_1 = \frac{2^{3/2} \pi n e^4 N_2 \omega_{vn} \omega_{nc} f_{vn} f_{nc}}{c m^{1/2} (\alpha_c + \alpha_v)^{3/2} \omega_1 \omega_2} \left[\frac{A^{1/2}}{B} + \frac{A^{1/2}}{C} \right], \quad (7)$$

"allowed-forbidden";

$$K_1 = \frac{2^{7/2} \pi n e^4 N_2 \omega_{vn} f_{vn}}{3c (m_T)^2 (\alpha_c + \alpha_v)^{5/2} \hbar \omega_1 \omega_2} \left[\frac{A^{3/2}}{B} + \frac{A^{3/2}}{C} \right], \quad (8)$$

"forbidden-forbidden";

$$K_1 = \frac{2^{11/2} \pi n e^4 m^{7/2} N_2}{9c (m_T)^4 (\alpha_c + \alpha_v)^{7/2} \hbar^2 \omega_1 \omega_2} \left[\frac{A^{5/2}}{B} + \frac{A^{5/2}}{C} \right], \quad (9)$$

where

$$\begin{aligned} A &= \hbar \omega_1 + \hbar \omega_2 - E_g, \\ B &= \left[\Delta E + \left(\frac{\alpha_n + \alpha_v}{\alpha_c + \alpha_v} \right) (\hbar \omega_1 + \hbar \omega_2 - E_g) - \hbar \omega_1 \right]^2, \\ C &= \left[\Delta E + \left(\frac{\alpha_n + \alpha_v}{\alpha_c + \alpha_v} \right) (\hbar \omega_1 + \hbar \omega_2 - E_g) - \hbar \omega_2 \right]^2. \end{aligned} \quad (10)$$

For the allowed-forbidden transition, it was assumed that the transition from the valence band to the intermediate state was allowed and that from the intermediate state to the conduction band was forbidden. In cases where the reverse is true, there will be a similar expression as Eq. (8) with ω_{vn} replaced by ω_{nc} and f_{vn}

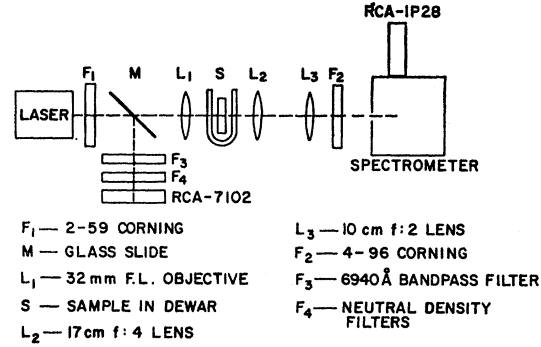


FIG. 2. Experimental arrangement for exiting double-photon absorption in CdS and observing the resulting radiative recombination. The outputs of the photomultipliers were fed directly into a dual-beam oscilloscope for comparison of the laser and fluorescence signals.

replaced by f_{nc} . In arriving at the above expressions, we have replaced the square of the sum of the matrix elements in Eq. (3) by the sum of squares which is equivalent to assuming that one is dealing with incoherent photons, since we are initially considering that the two photons $\hbar \omega_1$ and $\hbar \omega_2$ are produced by different sources. However, in the present experiments where the photons are of the same frequency and are derived from the same coherent source, the cross products of the matrix elements will make a small contribution to the transition probabilities. The double-photon absorption process employing a broad-band incoherent source of radiation can also be calculated from the above expressions by integrating over the spectral distribution below the band gap.

It is seen from Eqs. (7), (8), (9), and (10) that the absorption coefficient for photons $\hbar \omega_1$ is a function of the density N_2 of photons $\hbar \omega_2$ simultaneously present in the solid. The intensity-dependent absorption edges increase as some power of the photon energy depending upon the symmetries of the bands with a threshold at $\hbar \omega_1 + \hbar \omega_2 = E_g$. As a consequence of these characteristics, there are a number of different types of experiments which may be performed in order to detect the resultant electron-hole pairs created by two-photon absorption. These include the direct measurement of the intensity-dependent absorption, or the observation of photoconductivity, or fluorescence produced by irradiating a solid with photons of the same or different energies, both of which are less than the energy gap but whose sum is greater than the energy gap. For experimental convenience, the double-photon absorption at $\hbar \omega = 1.78$ eV was detected by observing the subsequent recombination emission in the region between 4900 and 5500 Å produced by the created pairs.

III. EXPERIMENTAL

The fluorescence spectrum was measured for a number of CdS crystals excited by a focused ruby laser whose

¹⁹ J. Bardeen, F. J. Blatt, and L. H. Hall, in *Proceedings of the Conference on Photoconductivity, Atlantic City, November 4-6, 1954*, edited by G. H. Breckenridge, B. R. Russell, and E. E. Hahn (John Wiley & Sons, Inc., New York, 1956), p. 146.

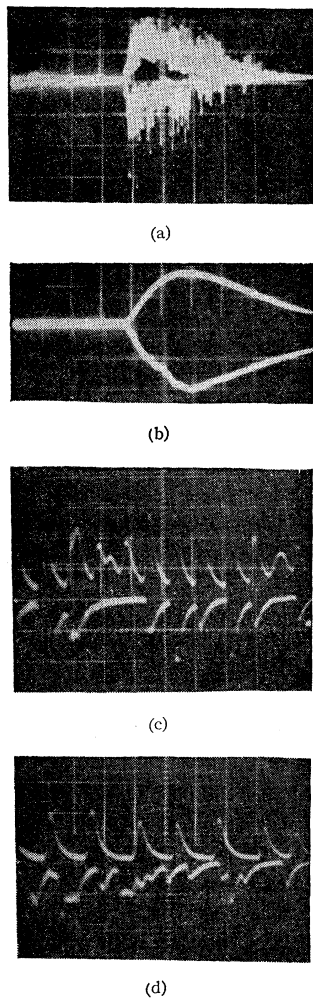


FIG. 3. Correlation between the emission of CdS at 123°K and the exciting ruby laser. In each figure the upper trace is the laser signal and the lower trace is the fluorescence signal; (a) emission at 4990 Å, horizontal sweep 100 $\mu\text{sec}/\text{cm}$; (b) same as (a) except for a larger time constant in detecting circuits; (c) same as for (a) but with horizontal sweep of 5 $\mu\text{sec}/\text{cm}$; (d) emission at 5100 Å same time constant as (a) but with horizontal sweep of 5 $\mu\text{sec}/\text{cm}$. Note the perfect time correlation in (c) for exciton recombination and the slightly delayed electron-impurity emission in (d).

photon energy $\hbar\omega = 1.78$ eV is less than the energy gap $E_g = 2.5$ eV, as well as by the conventional use of the 3660 Å Hg line, whose photon energy is greater than the energy gap. The spectral distribution as well as the intensity of the emission was determined as a function of incident intensity for both types of excitation. The spectra shown in this paper were for a typical undoped crystal of dimensions 10 mm \times 8 mm \times 1.78 mm grown at the RCA Laboratories; similar results were obtained using undoped crystals produced from other sources.

A schematic diagram of the experimental arrangement for observing the emission from crystals using the focused ruby laser is shown in Fig. 2. The ruby rod was 3 in. long and $\frac{1}{4}$ in. in diam with parallel ends coated with multilayer dielectric films giving 100% reflectivity on one face and 50% reflectivity on the other for the 6943 Å line. The ruby was mounted in a conventional laser head and was optically pumped by a helical GE FT-524 flash lamp. Operated at room temperature, this laser produced approximately 0.1 joules of output power which is equivalent to 4×10^{17} photons per flash. When focused onto an area of 10^{-2} cm² of the sample, the

photon density was $3 \times 10^{12}/\text{cm}^3$; larger energy densities produced by sharper focusing resulted in sample damage. The crystals were mounted in a Dewar which contained liquid nitrogen for the low temperature runs. The sample temperature was measured by an iron-constantan thermocouple cemented directly to the crystal. The spectra were measured by a Perkin-Elmer model 12C Spectrometer using a CaF₂ prism and utilizing an RCA 1P28 photomultiplier as a detector. The laser beam was monitored by reflecting part of the beam into an RCA 7102 photomultiplier. Filters F_1 and F_3 eliminated most of the xenon flash lamp radiation while F_2 attenuated the laser emission; their position in the optical chain is shown in Fig. 2.

In the studies of the emission excited by Hg excitation, a Bausch and Lomb monochromator using a 600 lines/mm grating was used. The HBO-500 mercury source was focused by a large aperture lens or mirror onto the crystals immersed in liquid nitrogen. The radiation, which was emitted from the same face of the crystal which received the excitation radiation was focused onto the monochromator slit after passing through appropriate filters. A Corning 7-54 filter and 10 cm of CuSO₄ solution isolated the 3660 Å Hg line. The emitted radiation was detected by an RCA 7265 photomultiplier whose output was fed to a recorder via a Vibron electrometer.

IV. RESULTS

The experimental results involve a comparison of the fluorescence spectra of CdS as excited by the 3660 Å Hg line with that excited by the 6943 Å ruby laser line. The emission spectrum was studied in the 4900- to 5500-Å region for both means of excitation since it is in this spectral region that previous single-quanta excited-fluorescence spectra have been extensively studied. The "green emission" bands in the region between 5100-5400 Å at 77°K have been previously identified as due to recombination of a free electron with a trapped hole,²⁰⁻²² while the so-called "blue emission" bands appearing at shorter wavelengths are presumably due to the recombination of free electron-hole pairs via an exciton state.²¹⁻²³ The emission was studied as a function of wavelength, time, polarization, and excitation intensity for the ruby excitation; and as a function of wavelength and excitation intensity for the Hg source.

A. Double-Photon Excited Emission

The correlation between the emission of CdS at 123°K and that of the exciting ruby laser is shown in Fig. 3. The detected output of the laser and the CdS emission were both displayed on separate channels of a Tektronix

²⁰ G. Diemer, G. J. van Gorp, and H. J. G. Meyer, *Physica* **23**, 987 (1957).

²¹ G. Diemer and A. J. Van der Houven van Oord, *Physica* **24**, 707 (1958).

²² R. J. Collins, *J. Appl. Phys.* **30**, 1135 (1959).

²³ D. G. Thomas and J. J. Hopfield, *Phys. Rev.* **116**, 573 (1959).

502 dual-beam oscilloscope. Figure 3(a) shows the partially resolved laser and emission spikes where it is seen that on the average the relative intensities are correlated with each other. This observation is further illustrated in Fig. 3(b) where a larger time constant in the detector circuits averaged the spikes. A time-expanded display of the laser and emission spikes is shown in Figs. 3(c) and 3(d). It should be noted that at 4990 Å, the region of exciton recombination, there is a perfect time correlation between exciton and emission spikes. In the region of electron-trapped hole recombination at 5100–5400 Å, there appears to be a time delay of several microseconds between the emission and the excitation spikes. The usefulness of using laser spikes for studying the kinetics of emission processes is clearly indicated by these results. Although there is no apparent correlation of the intensity of the excitation and emission spikes in the time expanded traces in Figs. 3(c) and 3(d), the correlation of the envelope of the laser and emission spikes previously indicated in Figs. 3(a) and 3(b) justifies the use of the envelope maxima as a measure of relative signal intensities. The lack of intensity correlation in the time expanded scale may be due to the detailed kinetics of the respective recombination processes.

The unpolarized and polarized emission spectra of a CdS crystal at 300°K excited by the laser is shown in Fig. 4. Previously, the CdS emission had only been observed at room temperature in a limited number of cases for excitation by photons greater than the energy gap.²⁴ The intensity of the emission varied from sample to sample for a given incident laser intensity; these

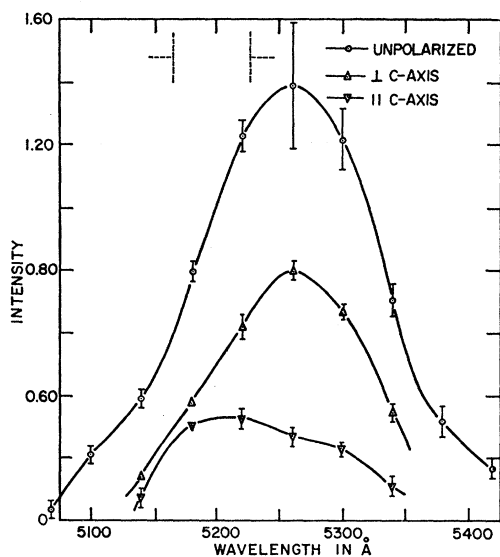


FIG. 4. Emission from CdS at 300°K excited by a focused ruby laser. The laser output was 0.17 J focused into a 10^{-2} cm² area of the crystal.

²⁴ B. A. Kulp, R. M. Detweiler, and W. A. Anders, Phys. Rev. 131, 2036 (1963).

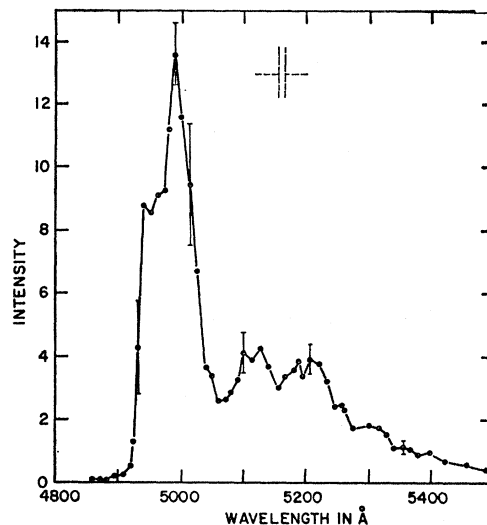


FIG. 5. Emission from CdS at 123°K excited by a ruby laser with 0.15 J focused into a 10^{-2} cm² area of the sample.

differences in quantum efficiencies are not surprising in the light of previous work on CdS. It is seen in Fig. 4 that the emitted radiation is polarized, the intensity perpendicular to the c axis is about three times that parallel to the axis. The recombination radiation was observed to follow the power law $I \propto I_0^{2 \pm 0.3}$ where I is the emission intensity and I_0 is the laser intensity. In obtaining these measurements, I_0 was varied by inserting neutral-density filters between the laser and the focusing lens. Each data point in Fig. 4 is the average of between two and five successive observations; the error lines indicate maximum deviations from this average. Since the laser intensity varied slightly from flash to flash, the observed emission intensities were normalized to the same laser intensity for all the recorded spectra. In the normalization procedure for this spectrum and all subsequent spectra reported in this work, the appropriate empirically determined power law relating the intensity of the emission to excitation was employed.

The above measurements were also performed at low temperatures where it was possible to observe fluorescence by ruby-laser excitation as well as by single-quanta Hg excitation for comparison. The observed unpolarized emission spectra at a temperature of 123°K is shown in Fig. 5. The rather large errors indicated in this spectrum make it difficult to ascribe some of the wiggles as due to real structure. However, successive runs enabled one to identify the major lines in this spectrum with the structure observed by using greater than band gap light; the line positions agree with those reported in the literature.^{22,23} The emission shown in Fig. 5 was found to be polarized with the component perpendicular to c axis being six times greater than the component parallel to the c axis.

Two groups of lines in the above spectrum exhibit

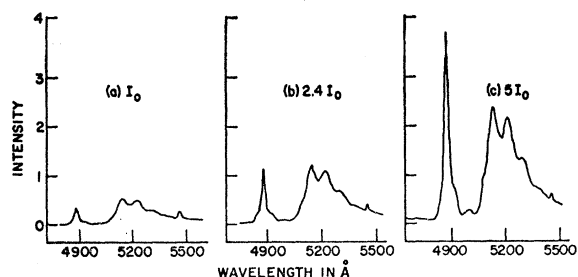


Fig. 6. Fluorescence spectra from CdS at 77°K as a function of incident intensity excited by the 3660-Å line of Hg.

different power laws relating the fluorescence to excitation intensity. Namely, the intensity of the lines between 4900 and 5050 Å varied as $I \propto I_0^{2 \pm 0.2}$ while for the lines between 5050 and 5400-Å the relationship is $I \propto I_0^{1 \pm 0.1}$. The emission obeyed these power laws over a range of I_0 of 10^2 . The significance of the difference will be discussed after similar relationships for the single-quanta excitation are presented.

B. Single-Photon Excitation

The unpolarized emission spectra at 77°K excited by the 3660-Å Hg line is shown in Fig. 6 for three different excitation intensities. There is a marked similarity between this single-photon excited spectra and the double-photon ruby laser excited spectra shown in Fig. 5. In general, the wavelengths observed for both means of excitation agree within experimental error. The major differences between the two spectra are with respect to the relative intensities of the various groups of lines. The failure of the intense 4875-Å band to appear in the laser-excited spectra is probably due to self-absorption in the sample since the emission was observed from the side opposite the incident laser beam. Double-photon absorption takes place essentially throughout the bulk of the solid and since the single-quanta absorption coefficient of CdS at 4875 Å is very large, the excited radiation at this wavelength will be self-absorbed. In contrast, for the case of the Hg excitation, the emission is collected from the same face as the incident excitation and so is generated close to the surface and can exit from the sample. The relative weakness of the 4940-, 4960-, and 4990-Å lines in the single-photon compared to the double-photon excited spectra is most likely due to the much smaller exciting intensity of the Hg source, relative to the effective double-photon pumping. A more detailed discussion of this point will be given later.

The different intensity law followed by the exciton recombination and the electron-trapped hole recombination is dramatically shown in Fig. 6 where it is seen that at low intensities the line at 4875 Å is weaker than the "green group" of lines at 5000-5400 Å while at high intensities it becomes larger than the latter group. The exciton lines at 4900-5000 Å follow the law $I \propto I_0^{1 \pm 0.1}$ while the "green" lines follow the relationship

$I \propto I_0^{0.6 \pm 0.05}$. This is to be contrasted with the power laws $I \propto I_0^{2 \pm 0.2}$ and $I \propto I_0^{1 \pm 0.1}$ for the corresponding lines in the double-photon excited spectra. The various power laws are shown in Fig. 7. The different intensity dependence for the exciton and electron-hole recombination is consistent with the previous observation by Diemer²¹ which was used by him to identify the respective recombination processes.

The quantum efficiency was measured at 77°K for the crystal used to obtain the spectra in Figs. 4 and 5 and was found to be approximately 0.1% for the 4990-Å line. The quantum efficiency is here defined as the ratio of the rate of emission to excitation since the intensity law for the 4990-Å line is approximately linear. The fluorescence yield for the front surface Hg excitation was found to be markedly dependent upon the surface treatment, while the double-photon yield was independent of this surface treatment. The above value of quantum efficiency was obtained for a well etched or cleaved surface.

We may summarize the experimental results shown in Figs. 4, 5, 6, and 7 by the observation that in general the spectra produced by both types of excitation are essentially similar except for differences in the emission intensity as a function of excitation intensity. The fact that the intensity of the emission spectra for the ruby-laser excitation increases within experimental error as the square of the corresponding Hg excitation over several decades for equivalent groups of lines strongly suggests that the former are due to double-photon absorption while the latter correspond to single-photon absorption.

C. Auxiliary Measurements

There are two alternate excitation mechanisms which could produce the observed fluorescence other than the

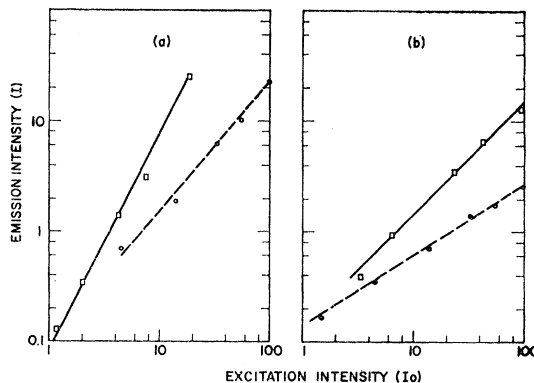


Fig. 7. Relative intensity of emission from CdS as a function of excitation intensity for both the Hg 3660 Å line and the ruby laser. In both figures the solid lines refer to laser excitation with crystal at 123°K while the dashed lines refer to Hg excitation at 77°K. (a) Emission of exciton recombination line at 4990 Å; (b) emission of electron impurity recombination at 5120 Å. Note that the emission follows a power law of the form $I \propto I_0^n$ where n for laser excitation is twice that for Hg excitation for each line.

creation of free electron-hole pairs by the simultaneous absorption of two laser photons via a virtual intermediate state. One is the self-absorption in the sample of a generated second harmonic $2\hbar\omega = 2 \times 1.78 \text{ eV} > E_g = 2.5 \text{ eV}$ and the consequent creation of an electron-hole pair by a final single-photon process. The second is two-photon absorption via an impurity state within the forbidden gap. In order to rule out these processes in the present experiments, the following auxiliary measurements were made.

As a consequence of the symmetry of the space group of CdS, (6 mm) one can easily show that if the laser beam is incident along the c axis no second harmonic should be generated. Consequently, if the observed emission depends on the absorption of second harmonic photons, there should be no emission for the above geometry. To check this point a CdS sample was cut from the same boule as was a previously studied crystal such that its c axis was perpendicular to its faces enabling the incident laser beam to be parallel to the c axis. At 300°K, this crystal exhibited the same intensity of recombination emission as the crystal whose c axis was perpendicular to the laser beam for the same excitation intensities. Hence one can disqualify the absorption of second harmonics of ruby as the fluorescence-excitation mechanism. It should be noted that the absence of second-harmonic generation applies strictly speaking only if the incident beam is parallel to the c axis. However the harmonic intensity for the convergent excitation employed would be too weak to be of any importance.

It has previously been shown that emission in CdS at 2.5 eV as well as at lower energies can be excited by photons having energies not exceeding 1.75 eV.^{25,26} These results were explained by considering a two-step optical-excitation process involving excited states of Cu impurity levels within the forbidden gap. In this process, a photon produces excitation to an excited level that has a reasonably long lifetime and then a second photon completes the excitation and is to be distinguished from double-photon absorption discussed above which involves the simultaneous absorption of two photons and is an intrinsic property of the solid. We found in agreement with the previous work²⁵ that tungsten excitation of our CdS crystals by photons having energies between 1.1 and 1.8 eV led to the same fluorescence as was observed with Hg excitation. However, we did not observe this emission for tungsten excitation for photon energies of 1.78 eV (the same as the laser) with a half-width of $\sim 0.02 \text{ eV}$. These results are contrary to the excitation curves obtained in the previous work²⁶ which substantiated the proposed two-photon excitation process via

²⁵ R. E. Halsted, E. F. Apple, J. S. Prener, Phys. Rev. Letters 2, 420 (1959).

²⁶ R. E. Halsted, E. F. Apple, J. S. Prener, and W. W. Piper, in *Proceedings of the International Conference on Semiconductor Physics, Prague, 1960* (Czechoslovakian Academy of Science, Prague, 1961).

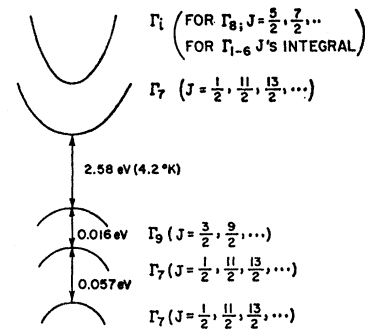


FIG. 8. The energy band structure of CdS at $\mathbf{k}=0$ with the associated band symmetries.

copper impurity levels. The intensities of emission for different crystals at 123°K obey the relationship $I \propto I_0^n$ with n constant for a given line over a number of decades for the laser excitation. It seems likely that a mechanism involving the replenishment of electrons from the initial copper level by the absorption of a second photon promoting electrons from the valence band to this copper level would lead to saturation effects over the range of excitation intensities of our experiments. The difference between our results for tungsten excitation and the previous work may lie in differences between our crystals and those employed in the above work.

V. DISCUSSION

We believe that the recombination radiation observed from CdS when excited by a ruby laser is a consequence of electron-hole pair creation by the simultaneous absorption of two red photons via a virtual intermediate state. The strongest experimental evidence for this conclusion follows from the detailed comparison of the fluorescence spectra as excited by the 3660-Å line of Hg, whose energy is greater than the band gap, with that produced by the 6943-Å laser line which is less than the band gap. The spectral distribution of the emission for both types of excitation are essentially similar, except for differences in the intensity dependence of the emission as a function of excitation intensity. The observed approximate quadratic dependency of the emission for laser excitation as compared with excitation by photon energies greater than the gap is to be expected if double-photon absorption were operative.

We shall now compare the observed fluorescence yields with the theory for double-photon absorption as further evidence that this excitation process can account for the observed spectra. The energy bands²⁷ for CdS at $\mathbf{k}=0$ are shown in Fig. 8 and the corresponding selection rules for double-photon absorption for electric dipole transitions at $\mathbf{k}=0$ are shown in Table I where the single-photon selection rules were used in the individual transitions.²⁸ In the present experiment, the final state in the conduction band is at $2 \times 1.78 \text{ eV}$, well above $\mathbf{k}=0$, and consequently it is not possible to

²⁷ Joseph L. Birman, Phys. Rev. 114, 1490 (1959).

²⁸ D. S. McClure, *Solid State Physics*, edited by F. Seitz and D. Turnbull (Academic Press Inc., New York, 1959), Vol. 9, p. 432.

TABLE I. Selection rules for double-quantum absorption in CdS for electric dipole transitions at $\mathbf{k}=0$.

Valence Band		Virtual Band		Conduction Band	Designation
Γ_9	\parallel	Γ_9	\perp	Γ_7	Allowed-allowed
Γ_9	\perp	Γ_7	\parallel, \perp	Γ_7	Allowed-allowed
Γ_9	\perp	Γ_8	f	Γ_7	Allowed-forbidden
Γ_9	f	Γ_{1-6}	f	Γ_7	Forbidden-forbidden
Γ_7	\parallel, \perp	Γ_7	\parallel, \perp	Γ_7	Allowed-allowed
Γ_7	\perp	Γ_9	\perp	Γ_7	Allowed-allowed
Γ_7	f	Γ_{1-6}, Γ_8	f	Γ_7	Forbidden-forbidden

ascribe a definite parity to the appropriate point in the Brillouin zone. Since we are primarily interested in an order of magnitude estimate of the absorption coefficient, we shall make the somewhat oversimplified, but reasonable assumption, that the CdS band structure can be represented by a spherical and parabolic three-band model as is shown in Fig. 1.

The expressions for "allowed-allowed" and "allowed-forbidden" transitions in Eqs. (7) and (8) will only be considered, since Eq. (9) for the "forbidden-forbidden" transitions yields much smaller values than are actually observed. In the above expressions, $\omega_1 = \omega_2 = 4 \times 10^{14}$ /sec, $E_g = 2.5$ eV, $m_T = m$, $f_{vn} = f_{nc} = 1$, $n = 2.6$ and $N_2 = 2 \times 10^{12}$ /cm³ for the present experiment. K_1 is rather insensitive to values of ΔE varying from 2.4 to 5.5 eV. The inverse effective-mass ratios for CdS were taken as $\alpha_c = 5$, $\alpha_v = 0.2$ and $\alpha_n = 1$. The first two values were obtained from optical-absorption experiments,²³ while the latter was assumed to be unity since the upper conduction band is expected to be a heavy mass band. Using the above values, Eqs. (7) and (8) give $K_1 = 2 \times 10^{-4}$ cm⁻¹ for the "allowed-allowed" transition and 4×10^{-6} cm⁻¹ for the "allowed-forbidden" case, respectively. If we use the experimentally determined quantum efficiency of 0.1% obtained from the single-photon Hg excitation of the 4990-Å line at 77°K, the calculated double-photon absorption coefficients predict corresponding fluorescence yields per laser flash of 8×10^9 photons and 2×10^8 photons for the respective transitions. The measured emission of the 4990-Å line at 123°K for laser excitation was 2×10^{11} photons at 123°K. This value has been corrected for an estimated loss factor of $\sim 10^3$ due to internal reflection losses in the sample and losses in coupling the output from the crystal into the spectrometer. It is seen that the observed value is in closer agreement with the calculated "allowed-allowed" rather than with the "allowed-forbidden" transitions. It was not possible to compare the room-temperature double-photon absorption signal with experiments since the inability to observe the single-photon emission at this temperature prevented the determination of the quantum efficiency.

The observation shown in Fig. 5 that the exciton emission lines are more intense relative to the electron-impurity recombination lines for double-photon laser excitation in contrast to the case for single-photon Hg

excitation shown in Fig. 6 can be understood from a consideration of the number of electron-hole pairs created by both sources. As we have seen, the exciton and impurity emission are proportional to $I_0^{1 \pm 0.1}$ and $I_0^{0.6 \pm 0.05}$, respectively, for single-photon excitation and to $I_0^{2 \pm 0.2}$ and $I_0^{1 \pm 0.1}$ for double-photon absorption; therefore for a sufficiently high excitation intensity the exciton emission should exceed the impurity emission. Although the double-photon absorption coefficient for the ruby is $\sim 2 \times 10^{-4}$ cm⁻¹, while for the Hg line the single-photon coefficient is $\sim 10^6$ cm⁻¹, the laser flux was 6×10^{22} photons/cm² sec while for the 3660-Å line of Hg it was 10^{13} photons/cm² sec; consequently approximately 10^4 more electron-hole pairs were created by the laser than the Hg source which is sufficient to explain the different relative intensities. Although the power laws for Hg and laser excitation were obtained for different effective-excitation intensities, the fact that the emission due to laser excitation is consistent with double-photon absorption for two different recombination processes indicates that the power laws shown in Fig. 7 would also hold for equal effective intensities of both sources.

One may regard the calculated double-photon absorption coefficients to be in reasonable agreement with experiment in view of the approximations made in its application to CdS and the experimental errors involved in determining the absolute fluorescence yield. The use of a three-band model with spherical and parabolic energy surfaces and the neglect of coherence effects and the effect of other conduction and valence bands could lead to appreciable errors in the estimates of the double-photon absorption coefficients. In addition, the theory should only be a good approximation in the vicinity of $\mathbf{k}=0$, whereas the final state for the double-photon observation of 1.78-eV photons was at much greater values of \mathbf{k} . The experimental yields may be in error by as much as a factor of 50 because of uncertainties in geometric factors which were used to calculate the yields.

The present experiment and theoretical estimates of double-photon absorption were merely intended as an order of magnitude check of this type of intrinsic-absorption process. These results suggest the feasibility of performing two-beam absorption experiments employing a fixed-frequency ($\hbar\omega_1$) high-intensity laser and a low-intensity variable-frequency ($\hbar\omega_2$) incoherent source where $\hbar\omega_1 < E_g/2$, $\hbar\omega_2 < E_g$ and $\hbar\omega_1 + \hbar\omega_2 > E_g$. The low-intensity source can be utilized since as we have shown previously, its absorption coefficient K_2 is proportional to the intensity of the intense source. This absorption coefficient can be measured directly or effectively by the subsequent fluorescence or photoconductivity. The frequency and polarization dependence of the absorption edge can yield information about the states involved in the virtual transitions by reference to Eqs. (7), (8), and (9) and the selection rules shown in Table I.

Double-photon absorption can be of use in a number

of optical studies. In cases where single-photon transitions between levels are forbidden for electric-dipole radiation, transitions can still be made by a double-photon process. In order to study transitions to states that have large absorption coefficients by single-photon absorption, one normally requires thin samples, or one performs reflectivity experiments which can be sensitive to surface treatment. The fact that photons of energy less than the band gap can produce transitions to states of twice the energy of the incident photon can be used to study upper states by the use of thick samples since the double-photon transitions take place throughout the bulk of the material.

[*Note added in proof.* The observation of a two-quantum absorption spectrum employing a high-intensity laser and a low-intensity variable-frequency incoherent light source in an experiment of the type suggested in this paper has been performed by J. J. Hopfield, J. M. Warlock, and Kwangjai Park, *Phys. Rev. Letters* **11**, 414 (1963) in KI.]

ACKNOWLEDGMENT

The authors wish to acknowledge the contribution of A. B. Dreeben for the samples used in this work and are grateful to D. A. Kramer for assistance in these measurements.

Effect of an External Electric Field on the Velocity of Sound in Semiconductors and Semimetals

HAROLD N. SPECTOR

Physics Division, IIT Research Institute, Chicago, Illinois

(Received 23 October 1963; revised manuscript received 23 December 1963)

A study is made of the effect of a dc electric field on the velocity of sound in semiconductors and semimetals. It is shown that the velocity of sound as a function of a dc field has either a maximum or minimum value at fields such that $V_d = S$. The particular cases studied are for acoustic waves propagating in an extrinsic semiconductor in a dc electric field and in a semimetal in crossed dc electric and magnetic fields.

I. INTRODUCTION

RECENTLY, interest has been centered on the amplification of acoustic waves via their interaction with conduction electrons in semiconductors and semimetals.¹⁻⁵ The amplification occurs when there are dc electric fields present which give the conduction electrons a net drift velocity, V_d , in the direction of propagation of the acoustic wave which exceeds the sound velocity S . Since the presence of the dc electric field has such a strong effect on the electron sound-wave interaction, it is of interest to see whether dc electric fields will also alter measurably the velocity of sound.

The effect of the interaction of the conduction electrons and the sound wave on the velocity of sound has been calculated by several authors⁶⁻⁹ in the absence of dc electric fields. However, most of these calculations

are only valid in metals where all the atoms are ionized. This is because they all depend upon the calculation of dispersion relations for the self-consistent electromagnetic field which is generated by the passage of the sound wave. In nonpiezoelectric semiconductors and semimetals, on the other hand, only a very small number of atoms are ionized and the major interaction between the conduction electrons and the sound wave is via deformation potential forces. These forces arise from the deformation of the electronic energy bands resulting from the passage of the sound wave. In this paper we will consider the interaction between the carriers and the sound wave as arising solely from the deformation potential.

In Sec. II, we shall develop a formalism for treating the influence of the electron-phonon interaction on the propagation of sound waves, which is valid both for extrinsic semiconductors and semimetals. In Sec. III and IV we shall treat, respectively, the cases of an extrinsic semiconductor in the presence of a dc electric field and of a semimetal in crossed electric and magnetic fields. In Sec. V we will discuss the possibility of observing the effects calculated in the paper.

II. GENERAL THEORY

We consider a longitudinal acoustic wave propagating in the x direction of a medium and we define a strain S ,

¹ A. R. Hutson, J. H. McFee, and D. L. White, *Phys. Rev. Letters* **7**, 237 (1961).

² W. P. Dumke and R. R. Haering, *Phys. Rev.* **126**, 1974 (1962).

³ A. M. Toxen and S. Tansal, *Phys. Rev. Letters* **10**, 481, (1963).

⁴ H. N. Spector, *Phys. Rev.* **127**, 1084, (1962); **130**, 910 (1963); **131**, 2512 (1963); **132**, 522 (1963).

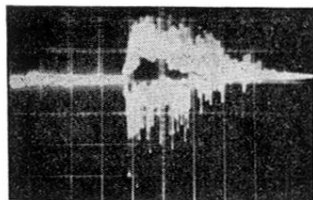
⁵ S. Eckstein, *Phys. Rev.* **131**, 1087 (1963).

⁶ N. Takimoto, *Progr. Theoret. Phys. (Kyoto)* **25**, 327, (1961).

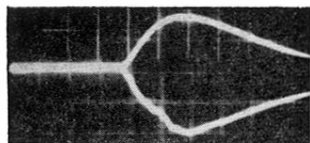
⁷ M. J. Harrison, *Phys. Rev. Letters* **9**, 299, (1962).

⁸ J. J. Quinn and S. Rodriguez, *Phys. Rev. Letters* **9**, 145 (1962).

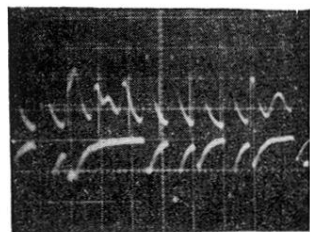
⁹ S. Rodriguez, *Phys. Letters* **2**, 271, (1962); *Phys. Rev.* **130**, 1778 (1963); *ibid.* **132**, 535 (1963).



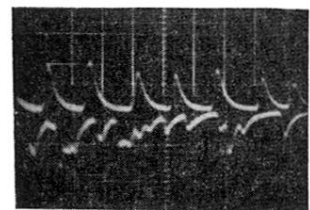
(a)



(b)



(c)



(d)

FIG. 3. Correlation between the emission of CdS at 123°K and the exciting ruby laser. In each figure the upper trace is the laser signal and the lower trace is the fluorescence signal; (a) emission at 4990 Å, horizontal sweep 100 μsec/cm; (b) same as (a) except for a larger time constant in detecting circuits; (c) same as for (a) but with horizontal sweep of 5 μsec/cm; (d) emission at 5100 Å same time constant as (a) but with horizontal sweep of 5 μsec/cm. Note the perfect time correlation in (c) for exciton recombination and the slightly delayed electron-impurity emission in (d).